RESEARCH ARTICLE

The *pro*-sequence of parathyroid hormone prevents premature amyloid fibril formation

Shubhra Sachan[1], Celia González Moya[1], Bruno Voigt[1] (iD), Marcel Köhn[2] and Jochen Balbach[1] (iD)

1 Institute of Physics, Biophysics, Martin-Luther-University Halle-Wittenberg, Germany
2 Medical Faculty, Martin-Luther-University Halle-Wittenberg, Germany

Correspondence

J. Balbach, Institute of Physics, Biophysics, Martin-Luther-University Halle-Wittenberg, Betty-Heimann-Str. 30, 06120 Halle, Germany
Tel: +49 345 28550
E-mail: jochen.balbach@physik.uni-halle.de

The parathyroid hormone (PTH) regulates the calcium and phosphate level in blood after secretion from parathyroid chief cells. The *pre*- and *pro*-sequences of precursor preproPTH get cleaved during PTH maturation. In secretory granules, PTH forms functional amyloids. Using thioflavin T fibrillation assays, circular dichroism, NMR spectroscopy, and cellular cAMP activation, we show that the *pro*-sequence prevents premature fibrillation by impairing primary nucleation because of Coulomb repulsion of positively charged residues. Under seeding or high salt conditions or in the presence of heparin at pH 5.5, proPTH fibril formation is delayed, but the monomer release properties are conserved. ProPTH can still activate *in cellulo* PTH receptor 1 but with impaired potency. These findings give some perspectives on medical applications of PTH in hormone therapy.

The human parathyroid hormone (PTH) is an 84 amino acid peptide hormone that is secreted by the parathyroid gland. The major function of the parathyroid hormone is to regulate calcium and phosphate homeostasis in blood by activating G protein-coupled receptors presented on the plasma membrane of bone and kidney cells [1]. The induced cascade *via* heterotrimeric G proteins converts the signal into a modulated flow of second messengers including cyclic AMP (cAMP), inositol triphosphate, diacylglycerol, or cGMP [2]. As these second messengers modulate skeletal, endocrine, cardiovascular, or nervous cell function [3], PTH_{1-84} and PTH_{1-34} are approved drugs against osteoporosis [4]. In PTH-secreting parathyroid tissue derived from both normal and overactive parathyroid glands, early studies identified intrafollicular amyloids [5]. In many cases, amyloid formation is associated with the onset of a pathological indication; however, an increasing number of amyloids are associated with physiological functions. One such example of functional amyloids is the storage of peptide hormones at a high concentration in membrane-coated secretory granules in the cytosol before release into the bloodstream [6]. PTH belongs to the latter class of peptides, which readily showed amyloid fibril formation also under *in vitro* conditions exhibiting a cross-β sheet rich conformation [7–9].

Many peptide hormones are initially synthesized as longer peptides with extra amino acid sequences present at the N-terminal region, which are proteolytically processed to yield active hormones. These precursors are further subdivided into *pre*-proteins and *pro*-proteins, where both precursors have a different function and processing kinetics [10]. One major step

towards a better understanding of the mechanism of *pro*-protein processing into a mature and biologically active protein has been the identification of a family of *pro*-protein convertases (PC) in the pathway of secretory proteins [11]. The PC family includes nine members: PC1/3, PC2, furin, PC4, PC5/6, PACE4 (paired basic amino acid cleaving enzyme 4), PC7, SKI-1/S1P (subtilisin kexin isozyme 1 also known as S1P) and PCSK9 (*pro*-protein convertase subtilisin kexin 9). The first seven members recognize and cleave precursor *pro*-proteins after the basic residue motif $(R/K)X_n(R/K)$ [12]. The eighth member, SKI-1 recognizes nonbasic residues after the C-terminal end of residues (R/K) X-(hydrophobic residue)-X (where X could be any amino acid except for proline and cysteine) [13]. PCSK9 undergoes an autocatalytic cleavage after the internal VFAQ^{152} stretch [14].

Accordingly, cellular formation of active parathyroid hormone (Fig. 1) occurs *via* two precursors preproPTH (115 amino acid) and proPTH (90 amino acid) [15]. The 25 amino acid *pre*-region acts as a signal sequence that directs the protein into cells' secretory pathway, whereas downstream to the signal sequence, the six amino acid *pro*-region acts as an adapter molecule, which supports the efficient and accurate functioning of the signal sequence [16]. The proteolytic conversion of preproPTH to proPTH takes place in the endoplasmic reticulum by signal peptidases and the conversion of proPTH to mature PTH takes place in the Golgi complex by proteolytic cleavage mediated by *pro*-protein convertases furin and PC7 [17–19]. Neither the calcium nor the dihydroxy vitamin D level in the extracellular fluid, which are the major regulators of parathyroid cell synthesis and secretory activity, influences the mRNA level of furin and PC7 [19]. This contrasts proinsulin processing by PC1 and PC2, which gets up-regulated in pancreatic beta-cells by glucose [20,21] Under physiological conditions, only mature PTH can be secreted by parathyroid chief cells and remaining prepro- and proPTH get degraded by the proteasome [22].

Besides its involvement in the chaperone- and proteasome-guided quality control during PTH maturation [22], not much is known about the role of the *pro*-sequence. Therefore, we characterized in this study the influence of the *pro*-sequence on the secondary structure of the hormone, on its *in vitro* fibril formation and *in cellulo* PTH receptor 1 activation. We found by NMR spectroscopy that the structure of proPTH corresponds to PTH. The *pro*-sequence, however, prevents premature fibrillation because of its four positive charges, which can be restored by furin cleavage, a high ionic strength, in the presence of heparin at acidic pH, and by seeding with sonicated PTH fibrils. Monomer release from proPTH fibrils is comparable to the release from PTH fibrils. The *pro*-sequence also reduces the PTH receptor 1 activation potency of proPTH by two orders of magnitude. For both effects, we discuss physiological implications.

Materials and methods

Protein expression and purification

Human PTH_{1-84} and $proPTH_{(-6)-84}$ proteins were cloned and purified according to previous protocols [23]. In brief, pET SUMO ADAPT vectors containing PTH or proPTH with a C-terminal His-tag were transformed into *Escherichia coli* BL21 (DE3) CodonPlus RIL cells. For NMR-based experiments, $^{15}N/^{13}C$ double labeling of the proteins was achieved in minimal media with $^{15}NH_4Cl$ as the sole nitrogen source and ^{13}C glucose as the sole carbon source. The SUMO fusion proteins were purified by Ni-NTA column chromatography followed by SUMO cleavage with the specific SUMO protease (1/100 ratio). Using hydrophobic interaction chromatography (HiTrap Butyl FF column), SUMO was separated from the protein of interest. Finally, both proteins were further purified by S-75 gel filtration chromatography.

Thioflavin T monitored kinetic fibrillation assay

ThT assays were carried out on a FLUOstar Omega (BMG Labtech GmbH, Ortenberg, Germany) reader using Greiner 96 F-bottom well plates (Greiner Bio-One GmbH, Frickenhausen, Germany). ThT fluorescence was monitored at 480 nm after excitation at 450 nm. All assays were performed with a protein concentration of 500 μM, at 37 °C, pH 7.4, and final sample volume of 150 μL. ThT fluorescence was collected every 300 s including a shaking time of 150 s (double orbital, 300 r.p.m.). ThT assays to compare the fibrillation kinetics of PTH and proPTH were recorded in standard fibrillation buffer, i.e., 50 mM sodium phosphate and 150 mM NaCl. Fibrillation kinetics for proPTH at different ionic strengths was performed at 50 mM sodium phosphate with varying amounts of NaCl viz. 0 M, 1 M, and 1.5 M. *Pro*-sequence cleavage was carried out by incubating 2 units of furin (P8077; NEB, Ipswich, MA, USA) per 150 μL of 500 μM proPTH. ThT assay to study the effect of *pro*-sequence cleavage on proPTH fibrillation kinetics was performed in a buffer comprising 100 mM HEPES, pH 7.4, 500 mM NaCl, furin, and 1 mM $CaCl_2$.

ThT assays to study fibrillation of PTH and proPTH at low pH conditions in the presence or absence of heparin were recorded in citrate buffer (20 mM, pH 5.5, 37 °C) and a protein concentration of 150 μM. Porcine intestinal heparin (molecular weight 20 kDa) was obtained from Carl

(A)

(B)

```
           -30          -20          -10          1          10           20          30
prepraPTH  M IPAKDMAKVM  IVMLAICFL  TKSDGKSVKKR  SVSEIQLMHN  LGKHLNSMER  VEWLRKKLQD
proPTH                      KSVKKR  SVSEIQLMHN  LGKHLNSMER  VEWLRKKLQD
PTH                                  SVSEIQLMHN  LGKHLNSMER  VEWLRKKLQD

                 40           50           60          70          80
preproPTH  VHNFVALGAP  LAPRDAGSQR  PRKKEDNVLV  ESHEKSLGEA  DKADVNVLTK  AKSQ
proPTH     VHNFVALGAP  LAPRDAGSQR  PRKKEDNVLV  ESHEKSLGEA  DKADVNVLTK  AKSQ
PTH        VHNFVALGAP  LAPRDAGSQR  PRKKEDNVLV  ESHEKSLGEA  DKADVNVLTK  AKSQ
```

Fig. 1. (A) Overview of the cellular maturation and target receptor activation of the parathyroid hormone. The *pre*-sequence guides translated preproPTH to the ER, where it gets cleaved by a signal peptidase. In the Golgi apparatus, furin or PC7 cleave the *pro*-sequence before mature PTH is secreted from membrane-coated granules into the blood. PTH receptor activation causes a second messenger modulation in target cells. During storage in secretory granules, PTH forms functional amyloid fibrils. (B) Amino acid sequence of preproPTH, proPTH (highlighted) and PTH.

Roth (Carl Roth GmbH, Karlsruhe, Germany) and used in a molar ratio of 1 : 1 (protein : heparin). All experiments were recorded in triplicates.

Seeded fibrillation

Seeds of PTH were prepared by sonication of PTH fibrils (500 μM) in 1.5 mL Eppendorf tubes by probe sonication (1 s pulse, 1 s pause, 15 × 10% amplitude). Fresh PTH

seeds were added to the reaction mixture directly before the start of the experiment. Final concentrations of seeds were 10 nM (2%) or 25 nM (5%). After 60 h the fibrillated samples were taken for EM investigation.

Transmission electron microscopy

The protein samples were diluted to a concentration of 25 μM and a 5 μL droplet of an individual fibril sample

was pipetted on the formvar carbon-coated copper grid (Plano GmbH, Wetzlar, Germany). The grid was then washed three times with 60 μL of water droplets. The residual water on the grid was removed with a Whatman filter paper. Grids were then stained with 30 μL of 1% (w/v) uranyl acetate, which was subsequently removed and the copper grids were then air-dried. Finally, TEM images were taken using an electron microscope (EM 900; Zeiss, Jena, Germany) at 80 kV acceleration voltage.

cAMP accumulation assay

HEK 293T cells stably expressing hPTHR1 were cultured at 37 °C in a 5% CO_2-humidified atmosphere. cAMP induction by PTH and proPTH was measured by cAMP-Gs dynamic HTRF kit from CisBio (Obrigheim, Germany). All working solutions were prepared according to the protocol provided by the vendor. Cells were washed twice with PBS, harvested by centrifugation (3000 g), and diluted to a density of 5×10^5 cells·mL^{-1} in stimulation buffer supplemented with 0.5 mM IBMX (3-isobutyl-1-methylxanthine). The cell suspension was then seeded at a density of 2500 cells per well into an HTRF 96 well low-volume white plate (5 μL·well^{-1}). Cells were then treated with 5 μL of a single concentration of peptide hormone per well, performed in triplicate. The plate was then sealed and incubated for 30 min at 37 °C. Five microliter of cAMP-d2 reagent working solution and 5 μL of cAMP Eu-Cryptate antibody working solution was then added into each well and incubated for 1 h at room temperature. Fluorescence measurement was taken using FLUOstar Omega with an advanced TRF optic head (excitation filter 337 nm, emission filters 620 and 665 nm, integration delay 60 μs, integration time 400 μs).

NMR spectroscopy

NMR experiments were performed on a Bruker Avance III 800 MHz spectrometer equipped with a CP-TCI cryoprobe at 25 °C. NMR samples contained 187 μM of double-labeled PTH or proPTH in 10 mM bis-tris buffer, pH 5.3. For backbone assignment standard double resonance experiment (^{15}N-HSQC) and triple resonance experiments (HNCACB, ^{15}N-TOCSY) were used. Spectra were processed with NMRPipe [24] and analyzed using NMRFAM-SPARKY [25]. For secondary structure analysis [26] the differences in ^{13}C$_\alpha$ and ^{13}C$_\beta$ from random coil values were taken from the chemical shift library based on Tamiola *et al.* [27].

CD spectroscopy

UV circular dichroism (CD) measurements were carried out on a Jasco J-810 spectrophotometer (Jasco Deutschland GmbH, Pfungstadt, Germany) using a 0.01 cm pathlength quartz cuvette (Hellma GmbH & Co. KG, Müllheim, Germany). PTH and proPTH concentration was adjusted to 20 μM in sodium phosphate (50 mM, pH 7.4) or citrate buffer (20 mM, pH 5.3). The scan speed was set to 50 nm·min^{-1} and collected spectra represent an average of 25 scans at 25 °C.

Monomer release assay

The monomer release from proPTH fibrils was performed in accordance with PTH fibrils [8]. ProPTH amyloid fibrils were achieved in a high salt buffer comprising 50 mM sodium phosphate and 1 M sodium chloride at pH 7.4. ProPTH concentration was kept at 500 μM. After completion of the fibrillation process the sample was centrifuged at 16 100 g. for 60 min to separate the amyloid fibrils (in the pellet) from monomeric protein (supernatant). The fibrils (in pellet) were then diluted and mixed in 1 mL buffer (50 mM sodium phosphate, 1 M sodium chloride, pH 7.4). This sample was incubated for 24 h at 37 °C and the amount of monomer released by the fibrils was determined by centrifugation of the sample followed by measurement of UV absorption of the supernatant fraction at 280 nm.

Results

Secondary structure of proPTH

At the N-terminus of PTH, residues N16-F34 are responsible for binding to the ECD domain (extracellular domain) of PTH receptors 1 and 2, and residues S1-H14 activate the receptor by binding and penetrating the extracellular loops 2, 3, and 4 out of the seven trans-membrane helices [3,28–30]. Both sections form an α-helical conformation in the receptor-bound state. In the unbound state, these sections have a transient propensity to form α-helices as judged by NMR and CD spectroscopy [8,31]. At pH 7.4, the CD spectrum of proPTH (Fig. 2A, black) resembles the spectrum of PTH [8] (Fig. 2A, red) reporting α-helical (negative ellipticity at 222 nm) and random coil (shift towards lower wavelengths than 208 nm) contributions. Also at pH 5.3, the CD spectrum of proPTH resembles that of PTH (Fig. 2B).

For a residue-resolved evaluation of the influence of the *pro*-sequence, the backbone and C$_\beta$ NMR chemical shifts of proPTH had been assigned by standard triple resonance experiments. The difference in the chemical shift deviation from random coil values [27] of the C$_\alpha$ and C$_\beta$ nuclei ($\Delta C_\alpha - \Delta C_\beta$) is an established measure of secondary structure sections along the polypeptide chain [26]. As expected, PTH shows segments of positive ($\Delta C_\alpha - \Delta C_\beta$) values for the N-terminal residues with highest values between S17 and Q29 (Fig. 2C) indicative of α-helical conformations. The transient character of these α-helical sections is reflected in the
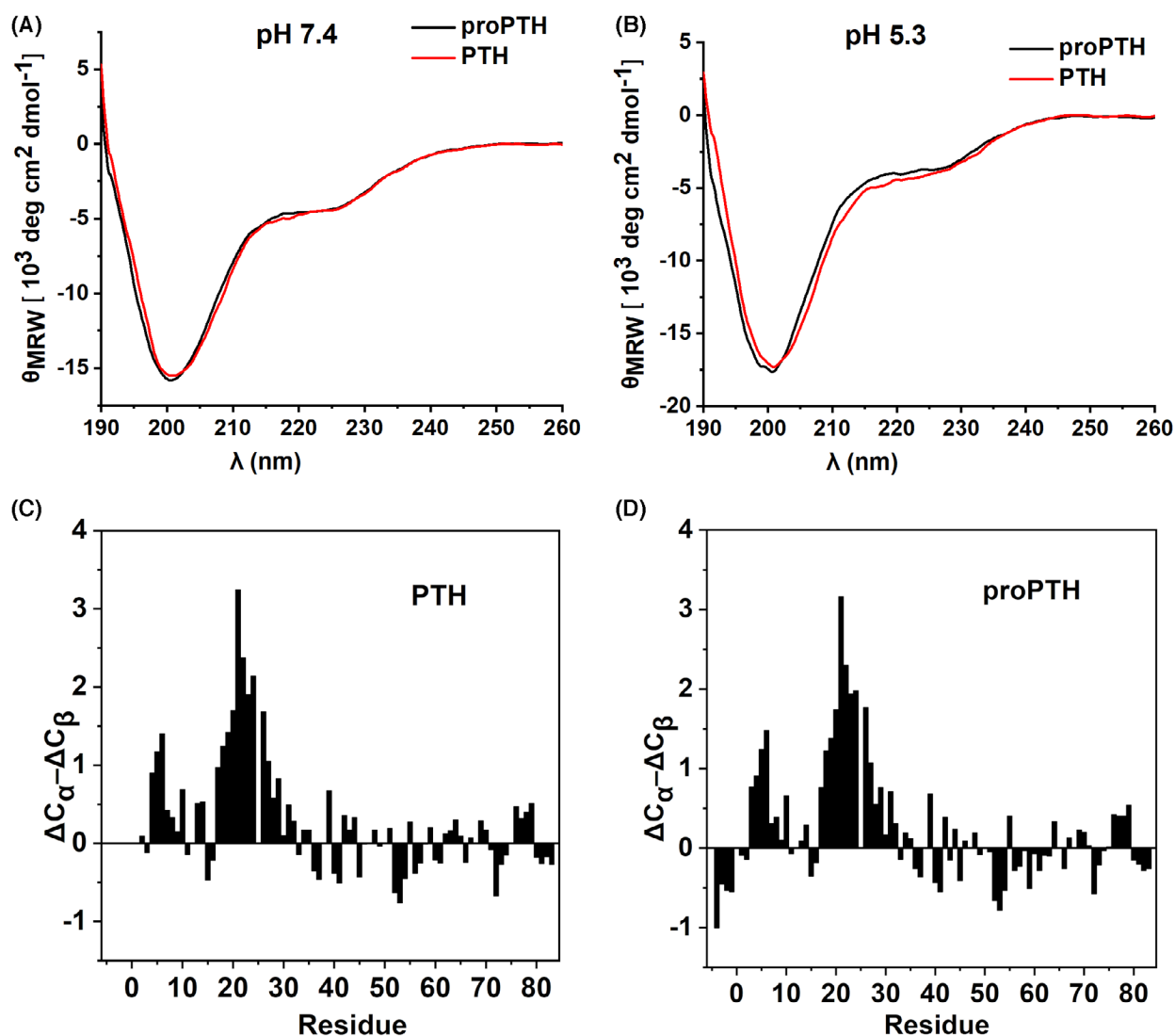
Fig. 2. Secondary structure characterization of PTH and proPTH. Circular dichroism spectrum of PTH (red) and proPTH (black) at (A) pH 7.4 and (B) pH 5.3. Protein concentration was adjusted to 20 μM in sodium phosphate (50 mM, pH 7.4) or citrate buffer (20 mM, pH 5.3). Differences in the NMR chemical shift deviations from random coil values are depicted for (C) PTH and (D) proPTH.

absolute values of this chemical shift parameter, which is below 2 for most residues. Permanently formed α-helices reach values up to 4 [32]. The ($\Delta C_\alpha - \Delta C_\beta$) values for residues D30 – Q84 confirm the intrinsically disordered section of PTH. In proPTH, this pattern remains unaffected (Fig. 2D) indicating that the *pro*-sequence does not influence the secondary structure propensities of unbound PTH.

Pro-sequence prevents fibrillation of PTH

Next, we asked the question to what extent the four positively charged side chains of the *pro*-sequence KSVKKR could affect the fibril formation of PTH.

Therefore, ThT fibrillation assays were recorded under identical buffer conditions (50 mM sodium phosphate, 150 mM NaCl, pH 7.4, 37 °C) and protein concentrations of 500 μM for PTH and proPTH. As expected from our previous reports [7,8], PTH forms amyloid fibrils indicated by a sigmoidal increase in the ThT fluorescence within 120 h and curvilinear fibrils in negatively stained electron micrographs (Fig. 3A red curves and C). By contrast, proPTH did not form fibrils according to both a missing sigmoidal ThT increase and no fibrillar structures in the electron micrographs (Fig. 3A black curves and B).

In the cellular context, the *pro*-sequence of proPTH gets enzymatically cleaved by propeptide convertases.
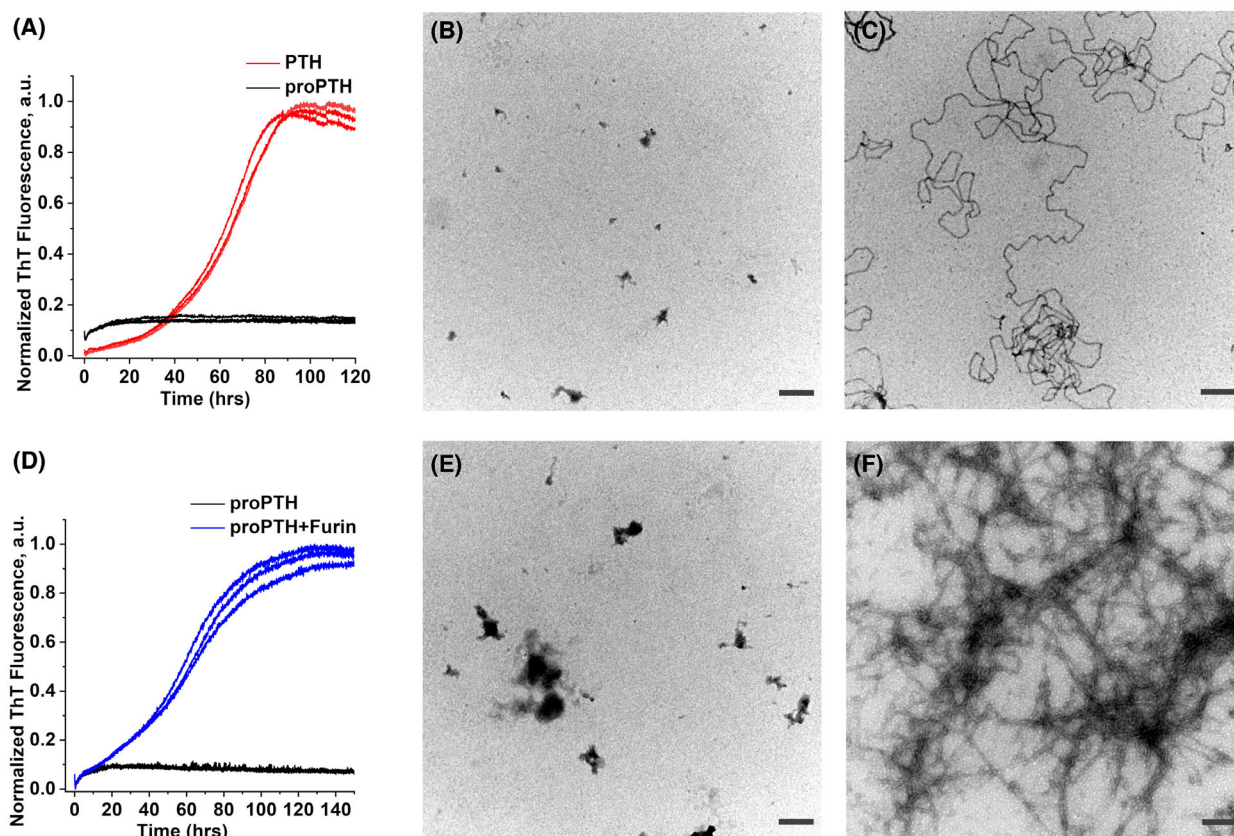
Fig. 3. Pro-sequence inhibits fibril formation. (A) Thioflavin T binding kinetics of PTH (red) and proPTH (black) in 50 mM sodium phosphate and 150 mM NaCl, pH 7.4, 37 °C. Transmission electron micrographs of the (B) proPTH and (C) PTH sample after completion of fibrillation assay. (D) Thioflavin T binding kinetics of proPTH in the absence (black) and presence (blue) of propeptide convertase furin in 100 mM HEPES, pH 7.4, 500 mM NaCl and 1 mM CaCl$_2$. Transmission electron micrograph after completion of the fibrillation assay of proPTH (E) in the absence and (F) in the presence of furin. Each experimental condition was investigated by three independent replicates. The scale bar in all micrographs corresponds to 0.2 μm.

Therefore, we added the convertase furin at the very beginning of the Thioflavin T monitored kinetic fibrillation assay of proPTH under our *in vitro* conditions. A sigmoidal increase for the ThT fluorescence was observed (blue curve in Fig. 3D) indicating that the released mature PTH after cleavage of the *pro*-sequence became fibrillation competent. Electron micrographs after completion of the fibrillation kinetics showed only fibrils for cleaved PTH and not for proPTH (Fig. 3E,F). In control experiments, furin had no influence on the ThT fibrillation kinetics of PTH (Fig. S4).

Fibrillation of proPTH under high salt or seeding conditions

One explanation for the suppression of fibril formation by the *pro*-sequence is the coulomb repulsion of its four positive charges, which might impair the association

reaction of PTH monomers. Therefore, this charge effect was screened by increasing the ionic strength of the buffer. With increasing NaCl concentrations up to 1.5 M, fibril formation in proPTH with a decreasing lag phase could be restored as evidenced by the respective ThT assay depicted in Fig. 4B. The corresponding EM micrographs after 250 h of fibrillation showed that proPTH forms curvilinear fibrils only under high salt conditions (Fig. 4G). To confirm that the *pro*-sequence makes the difference, fibrillation of PTH was performed under the identical 0 M salt conditions again leading to EM detectable fibrils (Fig. 4D). With increasing salt concentrations, the lag phase of PTH fibrillation becomes shorter (Fig. 4A). Comparing the time window required to get fibrils for proPTH and PTH under high salt conditions shows that the *pro*-sequence increases the lag phase at least by a factor of 4.

The mechanism of PTH fibrillation (to be published elsewhere) includes primary and secondary nucleation
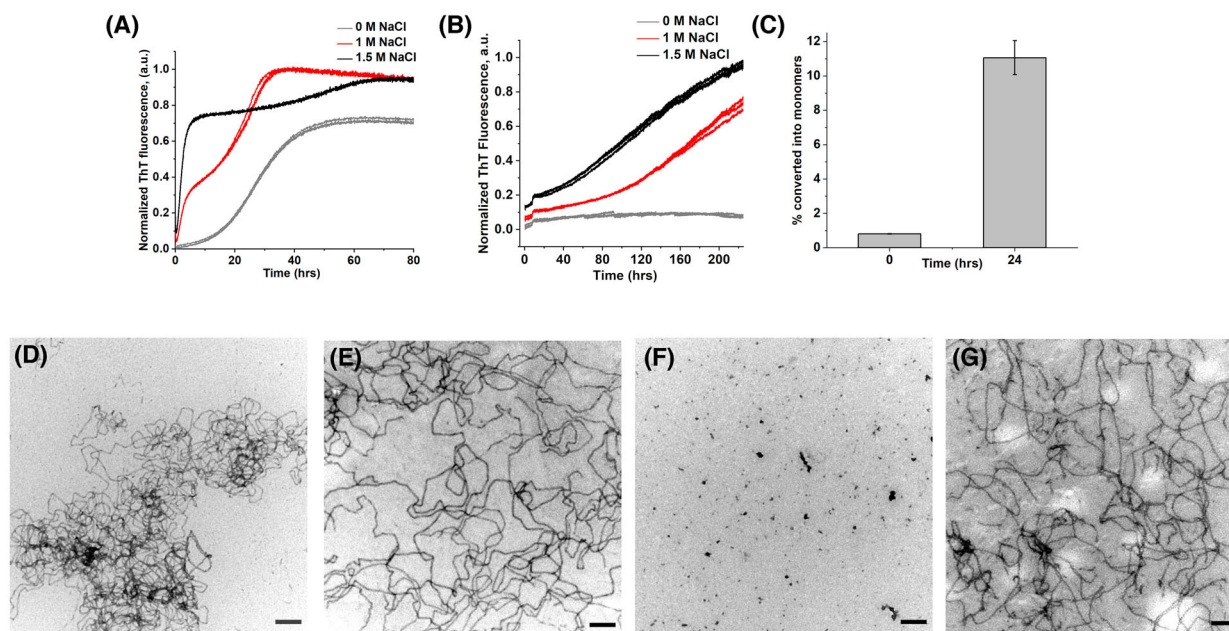
Fig. 4. Salt-dependent fibrillation kinetics and EM micrographs of PTH and proPTH. Thioflavin T binding assay of (A) PTH and (B) proPTH in 50 mM sodium phosphate at 37 °C, pH 7.4, and various NaCl concentrations: gray 0 M, red 1 M, black 1.5 M. Each experimental condition was investigated by three independent replicates. (C) Release of monomeric proPTH from fibrils of proPTH formed in the high salt buffer of 1 M NaCl upon dilution. The EM micrographs were taken from samples of (D) PTH in 0 M NaCl, (E) PTH in 1.5 M NaCl, (F) proPTH in 0 M NaCl, (G) proPTH in 1.5 M NaCl. The scale bar in all micrographs corresponds to 0.2 μm.

events and monomer inhibition. To elucidate the role of the *pro*-sequence during these processes, we performed seeding experiments with sonicated seeds derived from PTH fibrils (Fig. 5). Increasing amounts of seeds up to 5% reduced the lag time of PTH fibrillation during which primary nuclei form and foster fibril mass generation by secondary nucleation (Fig. 5A).

Adding the same prepared seeds to proPTH at low salt conditions, where no fibrils will form according to the ThT assay (red curve in Fig. 5B), fibril formation was observed (blue and black curve in Fig. 5B). In these experiments, no significant lag phase was detected. We attribute the exponential growth of fibril mass to secondary nucleation at the surface of the provided seeds. The final curvilinear fibril morphology of PTH and proPTH was indistinguishable in the corresponding electron micrographs (Fig. 5C,D). As proPTH showed in ThT assays without seeding only fibril formation under high salt conditions and then with a lag phase (Fig. 4B), we suggest that charge screening of the *pro*-sequence facilitate primary nucleation. Together, we propose that the *pro*-sequence under physiological salt concentrations prevents the formation of primary nuclei as starting point of fibril formation.

proPTH under physiological conditions

The last step of the secretory pathway of the parathyroid hormone is the controlled release into the bloodstream (Fig. 1). Therefore, fibril formation of PTH has to be a reversible process. In earlier studies, we showed that upon dilution indeed monomers are released from PTH fibrils and when equilibrium had reached after 24 h about 10% of monomers had dissolved [8]. To see how the *pro*-sequence might impair this equilibrium, we performed this experiment with proPTH fibrils. We found upon dilution that about 11% of monomeric proPTH got released within 24 h from proPTH fibrils (Fig. 4C).

During secretion and maturation of PTH the physiological pH drops from neutral values in the ER to values of about 5.5 in the trans-Golgi apparatus and secretory granules. For PTH, we found in a previous study that no fibrils are formed under these acidic conditions, but the presence of heparin could facilitate fibril formation [9]. Polyanionic heparin belongs to the family of glycosaminoglycans abundant in secretory granules and amyloid fibril deposits of peptide hormones [6]. Both PTH and proPTH did not show fibril formation in ThT assays at pH 5.5 (Fig. S3). The addition of equimolar amounts of heparin stimulated fibril formation and the sigmoidal kinetics reached a
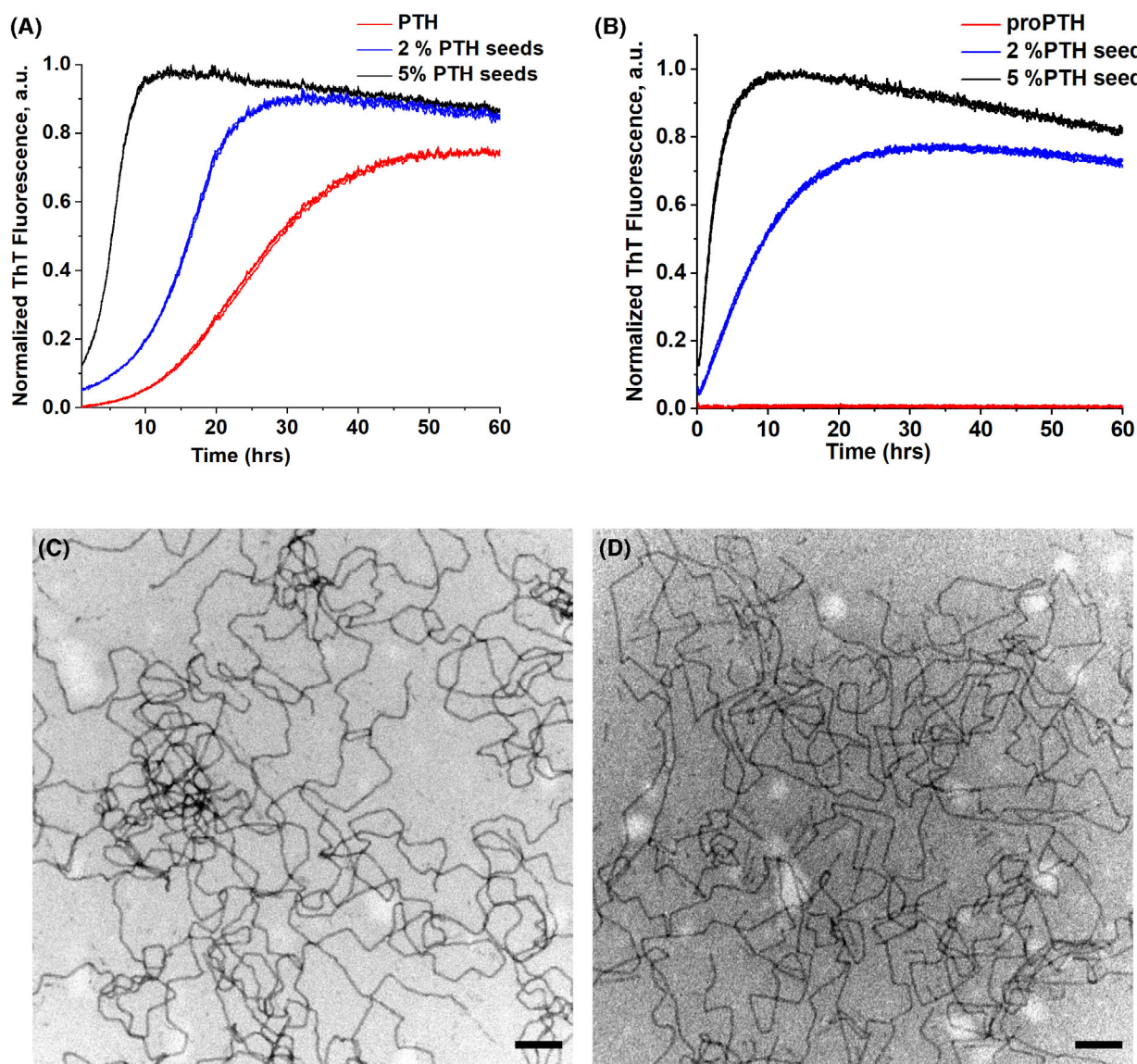
Fig. 5. Seeded fibrillation kinetics of proPTH and PTH. (A) Thioflavin T binding assay of PTH in absence of PTH seeds (red), 2 percent PTH seeds (blue), and 5 percent PTH seeds (black). (B) Thioflavin T binding assay of proPTH in absence of PTH seeds (red), 2 percent PTH seeds (blue), and 5 percent PTH seeds (black). EM micrograph of (C) PTH and (D) proPTH in presence of 2 percent PTH seed. Standard buffer conditions were used and each experimental condition was investigated by three independent replicates. The scale bar in all micrographs corresponds to 0.2 µm.

plateau after 1 h for PTH and after 4 h for proPTH. The curvilinear morphology of proPTH fibrils found in electron micrographs corresponds to the findings in the absence of heparin. These comparisons show that the *pro*-sequence retards fibril formation also under close physiological conditions.

In-cell cAMP activation by PTH and proPTH

The targets of PTH hormone released into blood from parathyroid glands are PTH receptors 1 and 2 (PTHR1 and PTHR2) in bone and kidney tissue. We employed the well-established cellular cAMP activation assay [33] to test the here investigated recombinant PTH and proPTH. In this assay, upon binding to the ligand, the increased cellular cAMP in HEK 293T cells stably expressing PTH receptor 1 competes with endogenous acceptor labeled cAMP for a donor labeled cAMP antibody. This competition changes the transfer efficiency of the donor-acceptor fluorescence resonance energy transfer (FRET) and thus the detected fluorescence emission at 665 nm. The cAMP
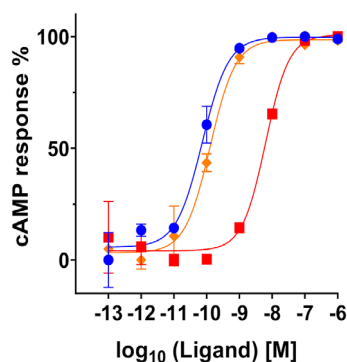
Fig. 6. *In cellulo* cAMP accumulation assay. PTH and proPTH induced cAMP accumulation in HEK 293T cells stably expressing wild-type PTHR1 receptors. The blue curve represents the cAMP response induced by PTH and the red curve by proPTH. For the orange curve, the PTH response was determined in the presence of 10^{-10} M proPTH. Symbols represent the mean of the performed assay in triplicate.

response depends on the extracellular hormone concentration and revealed for PTH a pEC_{50} value of 10.22 ± 0.13 (blue curve in Fig. 6) in very good agreement with literature values [33]. The corresponding experiment with proPTH showed nearly two orders of magnitude decrease in the potency of PTHR1 activation indicated by a pEC_{50} value of 8.27 ± 0.13 (red curve in Fig. 6).

This indicates that the *pro*-sequence at the N-terminus of PTH impairs the interactions with the trans-membrane part of the G protein-coupled PTH receptor 1. In a competition experiment, the assay of PTH-induced cAMP activation was repeated in the presence of 0.1 nM proPTH (orange curve in Fig. 6), revealing a pEC_{50} value of 9.8 ± 0.15. This reduction in potency shows that proPTH can compete with PTH for the same binding sites at the PTHR1 receptor.

Discussion

Pro-sequences fulfill a wide range of functions before being cleaved off during the maturation of proteins. This includes inhibition of proteases before reaching their final location [34], guidance during protein folding [35], as well as intra- and interchain disulfide bond mediated assembly of procollagen chains and protein stabilization [36]. In peptide hormones, the *pro*-sequence can also play an essential role as in the case of insulin, where the C-peptide assists in correct folding and disulfide bond formation between the A and the B chain of insulin before its cleavage [37].

Various *pro*-hormones, *pro*-neuropeptides, *pro*-transcription factors, pathogenic *pro*-proteins, *pro*-receptors, and other precursor proteins are substrates for the above-mentioned *pro*-protein convertases. Examples include progastrin, proglucagon, proANF, human proGLP1 (Glucagon-like peptide-1), and the here-studied human proPTH. Furin and PC7 are similar in their sequence specification to correctly process proPTH to PTH [11,38].

From the here presented results, we propose a new function of a *pro*-sequence, which is the prevention of premature formation of functional amyloid fibrils in the case of proPTH (Fig. 1). Under *in vitro* conditions of pH 7.4 and low salt, only mature PTH readily forms fibrils according to ThT kinetics and EM micrographs but not proPTH (Fig. 3A). Fibril formation of proPTH can be restored by cleaving the *pro*-sequence with furin (Fig. 3D). As proPTH cannot leave parathyroid cells even at high cellular concentrations after inhibition of its proteasomal degradation [18], we suspect that *pro*-sequence cleavage und subsequent fibril formation is obligatory for successful PTH secretion. The *pro*-sequence of PTH comprises residues KSVKKR. Four out of 6 residues have positively charged side chains, which lead to high local charge density near the fibril forming segment 25R–37L [8] of PTH that could abolish primary nucleation and fibril growth due to Coulomb repulsion. Therefore, no fibrillation could be observed for proPTH in buffer conditions under which PTH readily forms fibrils. Adding seeds from sonicated PTH fibrils allowed proPTH to form fibrils only *via* secondary nucleation supporting the hypothesis that the *pro*-sequence mainly prevents the formation of primary nuclei to start the fibrillation process. Under the acidic conditions corresponding to the secretory PTH granules, heparin is required to stimulate the fibrillation of both PTH and proPTH. This process is four times slower for proPTH compared with PTH, which shows that the retarding fibrillation property of the *pro*-sequence also remains under physiological conditions.

PTH fibrils readily release monomers [8], which is an essential requirement for hormone release from the secretory granules to the blood (Fig. 1) and for the classification as functional amyloids [6,39]. This main difference from pathogenic amyloids, which typically do not dissolve from deposits or plaques, is preserved for the proPTH fibrils formed in this study under high salt conditions because upon dilution, about 11% of monomeric proPTH got released within 24 h (Fig. 4C). Human peptide hormones such as corticotropin-releasing factor, β-endorphin, adrenocorticotropin, vasopressin, somatostatin, and prolactin

stored as functional amyloids in pituitary secretory granules revealed monomer release within the same time window in a comparable assay [6].

The NMR data show that the *pro*-sequence does not affect the secondary structure content of PTH both at pH 5.3 and 7.4. Both α-helix sections and the intrinsically disordered region are identical (Fig. 2) and both PTH and proPTH can induce cAMP in HEK293T cells stably expressing PTHR1 (Fig. 6). This contrasts the influence of post-translational modification of PTH by phosphorylation of S1, S3 and S17, which fully abolished receptor activation and the corresponding analysis of NMR chemical shift changes revealed that N-terminal residue up to position A36 sensed phosphorylation [33]. cAMP induction by proPTH is physiologically not very relevant, because only mature PTH will be released into the blood [18]. However, some mechanistic and pharmacological conclusions can be drawn. Two steps are required to activate the PTH receptors 1 and 2: binding of ligand to the extracellular domain (ECD) of the GPCR followed by its insertion into the trans-membrane helices (receptor J domain) [40]. The latter is facilitated by the N-terminal residues of PTH. The additional six residues of the *pro*-sequence probably interfere with this insertion, which could explain the 90fold reduction in activation potency (Fig. 6). For the ECD binding step we assume that the *pro*-sequence has a minor effect because more distant residues L15-F34 are involved and because proPTH could compete with PTH for the cAMP induction by binding the receptor (Fig. 6). Such competition between the *pro*-form and the mature form about a class B GPCR is also known for example for the bone morphogenic protein [41]. For proPTH the competition with PTH represents one perspective for drug development to treat hyperparathyroidism. As PTH_{1-84} and PTH_{1-34} and their formulations are already approved drugs for the treatment of osteoporosis [4] we anticipate that competing proPTH might serve as a compound for a proper blood level adjustment during hormone therapy. Functional amyloids of hormones had been put into perspective as a formulation of long-acting drugs [42]. Therefore, monomer-releasing proPTH fibrils formed under high salt concentrations might further support such a hormone therapy by serving as a hormone depot.

Acknowledgements

Author contributions

SS designed research, performed experiments, analyszed data, wrote the manuscript; CGM performed experiments and analysed data; BV supervised experiments, analysed data; MK supervised experiments, proofread the manuscript; JB designed research, supervised the project, wrote the manuscript.

Data accessibility

Data are available upon request from the authors.

References

1 Vilardaga J-P, Romero G, Friedman PA and Gardella TJ (2011) Molecular basis of parathyroid hormone receptor signaling and trafficking: a family B GPCR paradigm. *Cell Mol Life Sci* **68**, 1–13.

2 Lee M and Partridge NC (2009) Parathyroid hormone signaling in bone and kidney. *Curr Opin Nephrol Hypertens* **18**, 298–302.

3 Gardella TJ and Jüppner H (2001) Molecular properties of the PTH/PTHrP receptor. *Trends Endocrinol Metab* **12**, 210–217.

4 Kumar A and Balbach J (2022) Inactivation of parathyroid hormone: perspectives of drug discovery to combating hyperparathyroidism. *Curr Mol Pharmacol* **15**, 292–305.

5 Anderson T and Ewen S (1974) Amyloid in normal and pathological parathyroid glands. *J Clin Pathol* **27**, 656–663.

6 Maji SK, Perrin MH, Sawaya MR, Jessberger S, Vadodaria K, Rissman RA, Singru PS, Nilsson KPR, Simon R, Schubert D *et al.* (2009) Functional amyloids as natural storage of peptide hormones in pituitary secretory granules. *Science* **325**, 328–332.

7 Evgrafova Z, Voigt B, Baumann M, Stephani M, Binder WH and Balbach J (2019) Probing polymer chain conformation and fibril formation of peptide conjugates. *ChemPhysChem* **20**, 236–240.

8 Gopalswamy M, Kumar A, Adler J, Baumann M, Henze M, Kumar ST, Fändrich M, Scheidt HA, Huster D and Balbach J (2015) Structural characterization of

amyloid fibrils from the human parathyroid hormone. *Biochim Biophy Acta* **1854**, 249–257.

9 Lauth LM, Voigt B, Bhatia T, Machner L, Balbach J and Ott M (2022) Heparin promotes rapid fibrillation of the basic parathyroid hormone at physiological pH. *FEBS Lett* **596**, 2928–2939.

10 Docherty K (1982) Post-translational proteolysis in polypeptide hormone biosynthesis. *Annu Rev Physiol* **44**, 625–638.

11 Seidah NG, Mayer G, Zaid A, Rousselet E, Nassoury N, Poirier S, Essalmani R and Prat A (2008) The activation and physiological functions of the proprotein convertases. *Int J Biochem Cell Biol* **40**, 1111–1125.

12 Seidah NG and Chrétien M (1999) Proprotein and prohormone convertases: a family of subtilases generating diverse bioactive polypeptides. *Brain Res* **848**, 45–62.

13 Pasquato A, Pullikotil P, Asselin M-C, Vacatello M, Paolillo L, Ghezzo F, Basso F, di Bello C, Dettin M and Seidah NG (2006) The proprotein convertase SKI-1/S1P: in vitro analysis of Lassa virus glycoprotein-derived substrates and ex vivo validation of irreversible peptide inhibitors. *J Biol Chem* **281**, 23471–23481.

14 Benjannet S, Rhainds D, Essalmani R, Mayne J, Wickham L, Jin W, Asselin MC, Hamelin J, Varret M, Allard D *et al.* (2004) NARC-1/PCSK9 and its natural mutants: zymogen cleavage and effects on the low density lipoprotein (LDL) receptor and LDL cholesterol. *J Biol Chem* **279**, 48865–48875.

15 Kemper B, Habener JF, Mulligan RC, Potts JT Jr and Rich A (1974) Pre-proparathyroid hormone: a direct translation product of parathyroid messenger RNA. *Proc Natl Acad Sci USA* **71**, 3731–3735.

16 Wiren KM, Potts J and Kronenberg HM (1988) Importance of the propeptide sequence of human preproparathyroid hormone for signal sequence function. *J Biol Chem* **263**, 19771–19777.

17 Meyer DI, Krause E and Dobberstein B (1982) Secretory protein translocation across membranes—the role of the 'docking protein'. *Nature* **297**, 647–650.

18 Hendy GN, Bennett HP, Gibbs BF, Lazure C, Day R and Seidah NG (1995) Proparathyroid hormone is preferentially cleaved to parathyroid hormone by the prohormone convertase furin: a mass spectrometric study. *J Biol Chem* **270**, 9517–9525.

19 Canaff L, Bennett HP, Hou Y, Seidah NG and Hendy GN (1999) Proparathyroid hormone processing by the proprotein convertase-7: comparison with furin and assessment of modulation of parathyroid convertase messenger ribonucleic acid levels by calcium and 1, 25-dihydroxyvitamin D3. *Endocrinology* **140**, 3633–3642.

20 Alarcon C, Lincoln B and Rhodes C (1993) The biosynthesis of the subtilisin-related proprotein convertase PC3, but no that of the PC2 convertase, is regulated by glucose in parallel to proinsulin biosynthesis in rat pancreatic islets. *J Biol Chem* **268**, 4276–4280.

21 Martin SK, Carroll R, Benig M and Steiner DF (1994) Regulation by glucose of the biosynthesis of PC2, PC3 and proinsulin in (Ob/Ob) mouse islets of Langerhans. *FEBS Lett* **356**, 279–282.

22 Sakwe AM, Engström Å, Larsson M and Rask L (2002) Biosynthesis and secretion of parathyroid hormone are sensitive to proteasome inhibitors in dispersed bovine parathyroid cells. *J Biol Chem* **277**, 17687–17695.

23 Bosse-Doenecke E, Weininger U, Gopalswamy M, Balbach J, Knudsen SM and Rudolph R (2008) High yield production of recombinant native and modified peptides exemplified by ligands for G-protein coupled receptors. *Protein Expr Purif* **58**, 114–121.

24 Delaglio F, Grzesiek S, Vuister GW, Zhu G, Pfeifer J and Bax A (1995) NMRPipe: a multidimensional spectral processing system based on UNIX pipes. *J Biomol NMR* **6**, 277–293.

25 Lee W, Tonelli M and Markley JL (2015) NMRFAM-SPARKY: enhanced software for biomolecular NMR spectroscopy. *Bioinformatics* **31**, 1325–1327.

26 Luca S, Filippov DV, van Boom JH, Oschkinat H, de Groot HJ and Baldus M (2001) Secondary chemical shifts in immobilized peptides and proteins: a qualitative basis for structure refinement under magic angle spinning. *J Biomol NMR* **20**, 325–331.

27 Tamiola K, Acar B and Mulder FA (2010) Sequence-specific random coil chemical shifts of intrinsically disordered proteins. *J Am Chem Soc* **132**, 18000–18003.

28 Ehrenmann J, Schöppe J, Klenk C, Rappas M, Kummer L, Doré AS and Plückthun A (2018) High-resolution crystal structure of parathyroid hormone 1 receptor in complex with a peptide agonist. *Nat Struct Mol Biol* **25**, 1086–1092.

29 Zhao L-H, Ma S, Sutkeviciute I, Shen D-D, Zhou XE, de Waal PW, Li CY, Kang Y, Clark LJ, Jean-Alphonse FG *et al.* (2019) Structure and dynamics of the active human parathyroid hormone receptor-1. *Science* **364**, 148–153.

30 Pioszak AA and Xu HE (2008) Molecular recognition of parathyroid hormone by its G protein-coupled receptor. *Proc Natl Acad Sci USA* **105**, 5034–5039.

31 Marx UC, Adermann K, Bayer P, Forssmann W-G and Rösch P (2000) Solution structures of human parathyroid hormone fragments hPTH (1–34) and hPTH (1–39) and bovine parathyroid hormone fragment bPTH (1–37). *Biochem Biophys Res Commun* **267**, 213–220.

32 Gruber T, Lewitzky M, Machner L, Weininger U, Feller SM and Balbach J (2022) Macromolecular crowding induces a binding competent transient structure in intrinsically disordered Gab1. *J Mol Biol* **434**, 167407.

33 Kumar A, Gopalswamy M, Wishart C, Henze M, Eschen-Lippold L, Donnelly D and Balbach J (2014) N-terminal phosphorylation of parathyroid hormone (PTH) abolishes its receptor activity. *ACS Chem Biol* **9**, 2465–2470.

34 Bryan PN (2002) Prodomains and protein folding catalysis. *Chem Rev* **102**, 4805–4816.

35 Baker D, Shiau AK and Agard DA (1993) The role of pro regions in protein folding. *Curr Opin Cell Biol* **5**, 966–970.

36 Doyle SA and Smith BD (1998) Role of the pro-α2 (I) COOH-terminal region in assembly of type I collagen: disruption of two intramolecular disulfide bonds in pro-α2 (I) blocks assembly of type I collagen. *J Cell Biochem* **71**, 233–242.

37 Wahren J, Ekberg K, Johansson J, Henriksson M, Pramanik A, Johansson B-L, Rigler R and Jörnvall H (2000) Role of C-peptide in human physiology. *Am J Physiol Endocrinol Metab* **278**, E759–E768.

38 Munzer JS, Basak A, Zhong M, Mamarbachi A, Hamelin J, Savaria D, Lazure C, Hendy GN, Benjannet S, Chrétien M *et al.* (1997) In vitro characterization of the novel proprotein convertase PC7. *J Biol Chem* **272**, 19672–19681.

39 Sergeeva AV and Galkin AP (2020) Functional amyloids of eukaryotes: criteria, classification, and biological significance. *Curr Genet* **66**, 849–866.

40 Gardella T, Axelrod D, Rubin D, Keutmann HT, Potts JT Jr, Kronenberg H and Nussbaum SR (1991) Mutational analysis of the receptor-activating region of human parathyroid hormone. *J Biol Chem* **266**, 13141–13146.

41 Hauburger A, von Einem S, Schwaerzer GK, Buttstedt A, Zebisch M, Schräml M, Hortschansky P, Knaus P and Schwarz E (2009) The pro-form of BMP-2 interferes with BMP-2 signalling by competing with BMP-2 for IA receptor binding. *FEBS J* **276**, 6386–6398.

42 Maji SK, Schubert D, Rivier C, Lee S, Rivier JE and Riek R (2008) Amyloid as a depot for the formulation of long-acting drugs. *PLoS Biol* **6**, e17.

Supporting information

Additional supporting information may be found online in the Supporting Information section at the end of the article.

Fig. S1. 2D 1H-15N HSQC spectrum including sequence specific backbone resonance assignments of PTH.

Fig. S2. 2D 1H-15N HSQC spectrum including sequence specific backbone resonance assignments of proPTH.

Fig. S3. (A) ThT fibrillation assay PTH (blue) or proPTH (green) in the absence of heparin and in presence of 150 μM heparin of PTH (black) and proPTH (red) at 37 °C and pH 5.5 in 20 mM citrate buffer. Protein concentration is 150 μM. (B) Same fibrillation kinetics as in (A) of proPTH in presence (red) and absence of heparin (green) recorded for 5 h. (C) EM micrograph of fibril of proPTH achieved in presence of heparin after 5 h.

Fig. S4. Fibrillation of 500 μM PTH in presence and absence of furin at 37 °C in 100 mM HEPES, pH 7.4, 500 mM NaCl and 1 mM CaCl2.